

Supplementary information

Distorted octahedron-dependent red-emitting $\text{Li}_2\text{K}_4\text{TiOGe}_4\text{O}_{12}:\text{Mn}^{4+}$ phosphor for White LEDs

Haiyan Wu,^{a,b,c,d} Guang Zhu,^{*b} Jian Zhang,^{a,b} Hui Xie,^b Tao Tan,^{c,d} Yan Gao,^{*a} Lihong Jiang,^{*c} Chengyu Li,^{c,d} and Hongjie Zhang^c

^a Key Laboratory for Water Quality and Conservation of the Pearl River Delta, Institute of Environmental Research at Greater Bay Area, Guangzhou University, Ministry of Education, Guangzhou 510006, China

^b Key Laboratory of Spin Electron and Nanomaterials of Anhui Higher Education Institutes, Suzhou University, Suzhou 234000, China

^c State Key Laboratory of Rare Earth Resource Utilization, Changchun Institute of Applied Chemistry, Chinese Academy of Sciences, Changchun 130022, People's Republic of China

^d University of Science and Technology of China, Hefei 230026, People's Republic of China

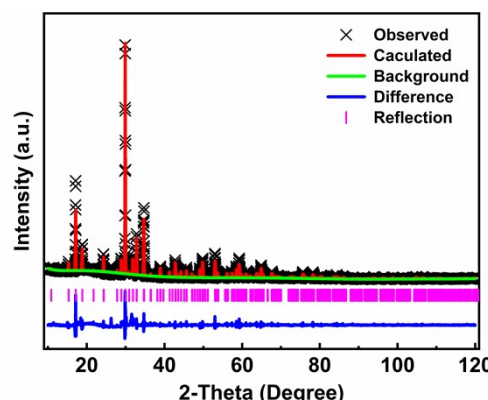


Fig. S1 XRD Rietveld refinement patterns of LKTGO.

Table S1. Rietveld fitting results of LKTGO and LKTGO:0.003Mn⁴⁺.

formula	LKTGO	LKTGO:0.003Mn ⁴⁺
crystal system	tetragonal	tetragonal
space group	$P4nc$	$P4nc$
a (Å)	11.5970(5)	11.62134(7)
b (Å)	11.5970(5)	11.62134(7)
c (Å)	5.1738(3)	5.184171(2)
$\alpha = \beta = \gamma$ (deg)	90	90
Z	2	2
V (Å ³)	695.82(8)	696.83(3)
R_p	0.0878	0.0708
R_{wp}	0.0998	0.0582
χ^2	14.04	6.888

Table S2. Atomic positions of LKTGO.

atom	x	y	z	occupancy	U _{iso}
Li	1	0.5	0.2729	1.000	0.0400
K	0.7662	0.9217	-0.0899	1.000	0.0160
Ti	1	1	0.4464	1.000	0.0043
Ge	0.7803	0.6084	-0.0603	1.000	0.0177
O1	0.8798	0.4827	-0.0984	1.000	0.0165
O2	0.6271	0.5904	0.0160	1.000	0.0837
O3	0.7670	0.6740	-0.3600	1.000	0.0583
O4	1	1	0.1132	1.000	0.0278

Table S3. Atomic positions of LKTGO:0.003Mn⁴⁺.

atom	x	y	z	occupancy	U _{iso}
Li	0.0000	0.5000	0.2511	1.0000	0.07778
K	0.7665	0.9225	-0.0710	1.0000	0.01812
Ti	1.0000	1.0000	0.3749	0.9948	0.00740
Ge	0.7816	0.6087	-0.0956	1.0000	0.01534
O1	0.8908	0.4810	-0.0500	1.0000	0.00681
O2	0.6302	0.5917	0.0124	1.0000	0.13379
O3	0.7542	0.6720	-0.3825	1.0000	0.06131
O4	1.0000	1.0000	0.7194	1.0000	0.00851
Mn	1.0000	1.0000	0.3749	0.0052	0.00740

Table S4. The calculated β_1 values and spectroscopic parameters of Mn⁴⁺ ions in various hosts.

Host	D _q	B	C	β_1	E (² E _g)	Ref
CaZrO ₃	1850	754	3173	0.983	15054	1
Ba ₂ GdNbO ₆	1931	855	2859	0.992	14793	2
CaAl ₁₂ O ₁₉	2132	807	3088	0.999	15244	3
SrGe ₄ O ₉	2362	832	3024	1.004	15267	4
Ca ₂ LaNbO ₆	1934	838	2827	0.976	14598	5
Sr ₂ MgGe ₂ O ₇	2387	833	2989	0.975	15175	6
La(MgTi) _{1/2} O ₃	2053	700	2959	0.915	14124	7
Mg ₂ Al ₄ Si ₅ O ₁₈	2141	927	2560	0.996	14705	8
K ₂ Ge ₄ O ₉	2163	785	3146	0.996	15281	9
CaMg ₂ La ₂ W ₂ O ₁₂	2088	731	2912	0.924	14124	10
LiAl ₅ O ₈	2014	725	2900	0.920	13977	11
YAlO ₃	2100	720	3025	0.938	14450	12
Y ₂ Sn ₂ O ₇	2100	700	3515	1.016	15563	13
SrMgAl ₁₀ O ₁₇	2237	791	3084	0.989	15152	14
YAl ₃ (BO ₃) ₄	1890	755	3015	0.956	14620	15
Li ₂ K ₄ TiOGe ₄ O ₁₂	2137	813	3007	0.990	15038	This work

Table S5. CIE coordinates of LKTGO:0.003Mn⁴⁺ at different temperature ($T = 298\text{--}473\text{ K}$).

Temperature (K)	CIE coordinates (x, y)
298	(0.719, 0.281)
323	(0.716, 0.283)
348	(0.711, 0.288)
373	(0.700, 0.298)
398	(0.676, 0.320)
423	(0.625, 0.366)
448	(0.552, 0.433)
473	(0.496, 0.484)

Table S6. The parameters of the prepared LED at various driving currents.

Current (mA)	Luminous efficiency (lm/W)
20	0.67
40	0.65
60	0.61
80	0.61
100	0.55
120	0.52
140	0.50
160	0.47
180	0.46
200	0.44
220	0.43
240	0.42
260	0.41
280	0.40
300	0.40

Table S7. The parameters of the prepared WLED at various driving currents.

Current (mA)	Luminous efficiency (lm/W)	CRI
20	56.89	90.20
30	56.20	88.52
40	55.08	87.60
50	54.06	86.08
60	53.66	84.80
70	52.88	83.28
80	52.02	81.30
90	51.66	80.08
100	51.23	78.60
110	50.12	77.08
120	50.11	75.56

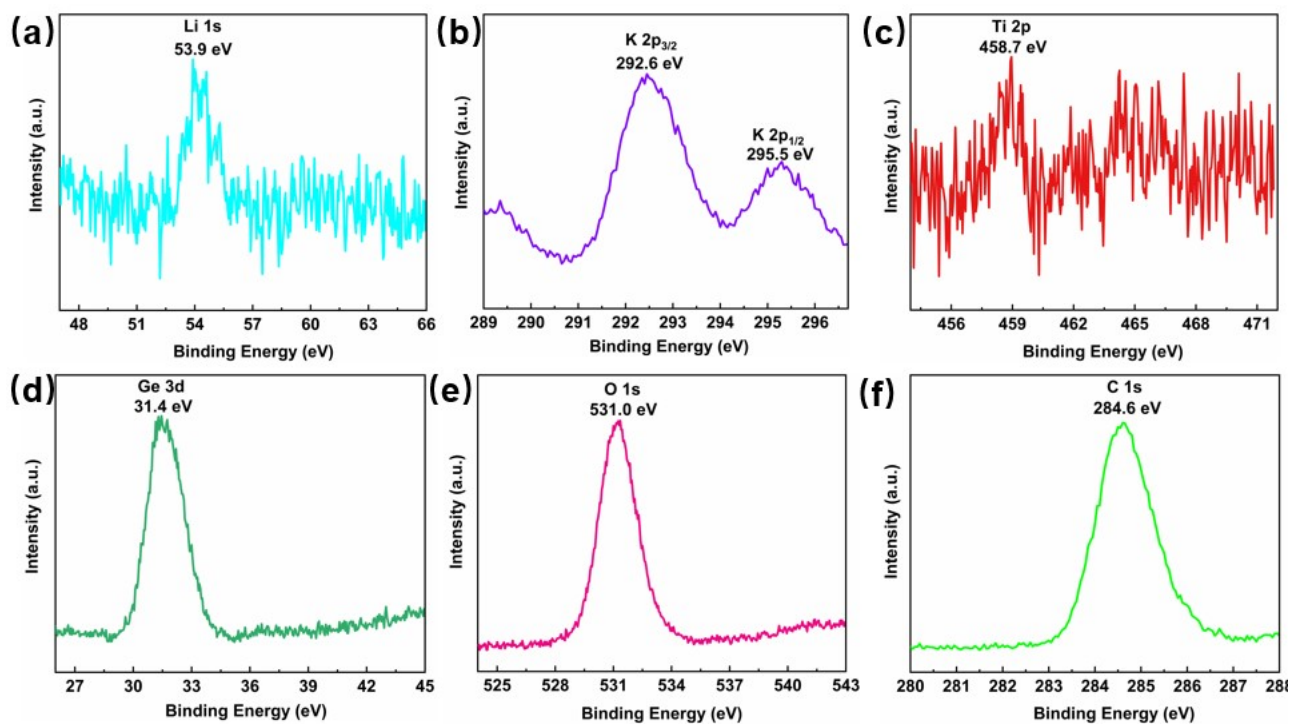


Fig. S2 XPS spectrogram of the LKTGO:0.003Mn⁴⁺ phosphors. (a) Li-1s, (b) K-2p, (c)Ti-2p, (d) Ge-3d, (e) O-1s and (f) C-1s.

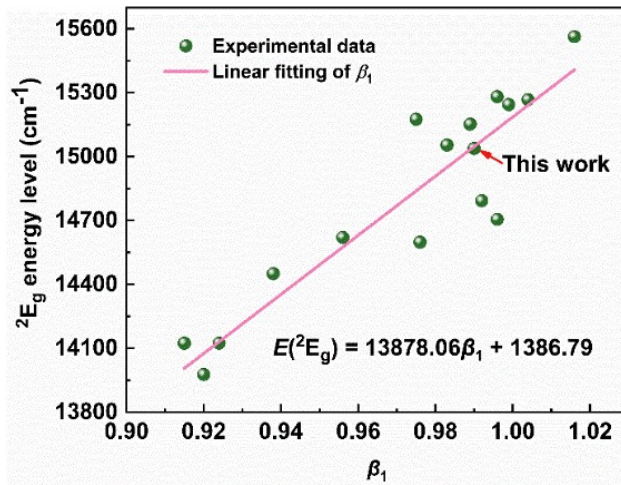


Fig. S3 Empirical relation between the nephelauxetic ratio β_1 and the energy position of the Mn^{4+} : ${}^2\text{E}_g$ state in octahedral complexes.

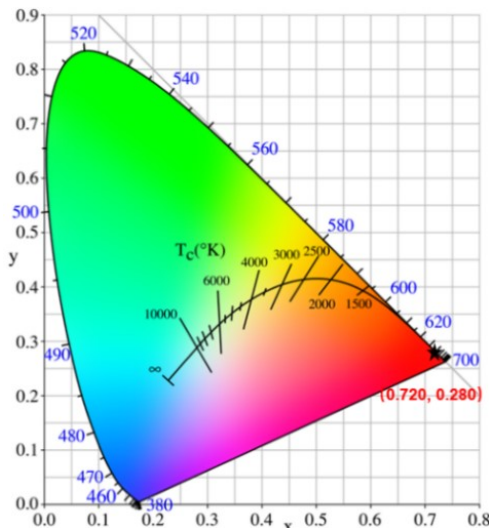


Fig. S4 CIE coordinates of LKTGO:0.003Mn⁴⁺ phosphors at room temperature ($T = 273$).

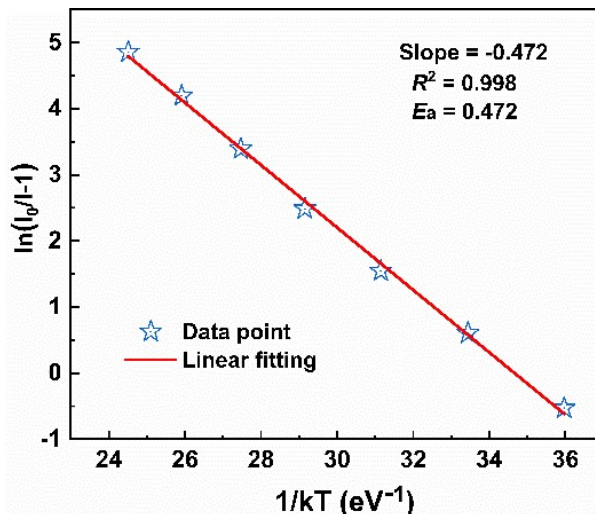


Fig. S5 The relationship of $\ln[(I_0/I_T)-1]$ with $1/T$ in LKTGO:xMn⁴⁺ phosphor.

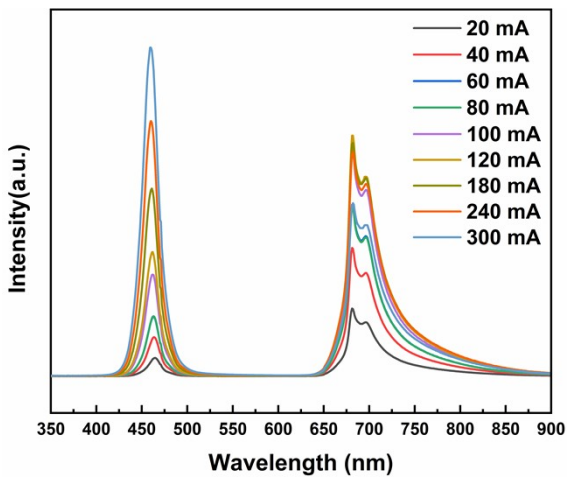


Fig. S6 PL spectra of the prepared LED at various driving currents.

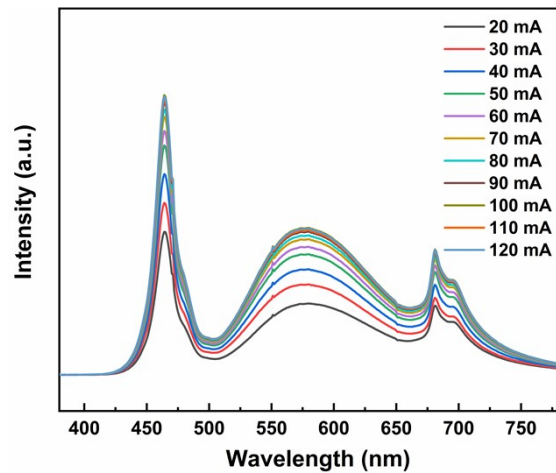


Fig. S7 PL spectra of the prepared WLED at various driving currents.

References

1. M. G. Brik and A. M. Srivastava, Electronic Energy Levels of the Mn⁴⁺ Ion in the Perovskite, CaZrO₃, *ECS J. Solid State Sci. Technol.*, 2013, **2**, R148-R152.
2. A. Fu, C. Zhou, Q. Chen, Z. Lu, T. Huang, H. Wang and L. Zhou, Preparation and optical properties of a novel double-perovskite phosphor, Ba₂GdNbO₆:Mn⁴⁺, for light-emitting diodes, *Ceram. Int.*, 2017, **43**, 6353-6362.
3. T. Murata, T. Tanoue, M. Iwasaki, K. Morinaga and T. Hase, Fluorescence properties of Mn⁴⁺ in CaAl₁₂O₁₉ compounds as red-emitting phosphor for white LED, *J. Lumin.*, 2005, **114**, 207-212.
4. S. J. Kim, H. S. Jang, S. Unithrattil, Y. H. Kim and W. B. Im, Structural and luminescent properties of red-emitting SrGe₄O₉:Mn⁴⁺ phosphors for white light-emitting diodes with high color

- rendering index, *J. Lumin.*, 2016, **172**, 99-104.
5. L. Shi, Y.-j. Han, Z.-x. Ji, Z.-h. Li, H.-h. Li, J.-y. Zhang and Z.-w. Zhang, Synthesis and photoluminescence properties of a novel $\text{Ca}_2\text{LaNbO}_6:\text{Mn}^{4+}$ double perovskite phosphor for plant growth LEDs, *J. Mater. Sci. Mater. Electron.*, 2019, **30**, 15504-15511.
6. W. Chen, Y. Cheng, L. Shen, C. Shen, X. Liang and W. Xiang, Red-emitting $\text{Sr}_2\text{MgGe}_2\text{O}_7:\text{Mn}^{4+}$ phosphors: Structure, luminescence properties, and application in warm white light emitting diodes, *J. Alloys Compound.*, 2018, **762**, 688-696.
7. Z. Zhou, J. Zheng, R. Shi, N. Zhang, J. Chen, R. Zhang, H. Suo, E. M. Goldys and C. Guo, Ab Initio Site Occupancy and Far-Red Emission of Mn^{4+} in Cubic-Phase $\text{La}(\text{MgTi})_{1/2}\text{O}_3$ for Plant Cultivation, *ACS Appl. Mater. Interfaces*, 2017, **9**, 6177-6185.
8. A. Fu, L. Zhou, S. Wang and Y. Li, Preparation, structural and optical characteristics of a deep red-emitting $\text{Mg}_2\text{Al}_4\text{Si}_5\text{O}_{18}:\text{Mn}^{4+}$ phosphor for warm w-LEDs, *Dyes Pigments*, 2018, **148**, 9-15.
9. F. Baur and T. Jüstel, Dependence of the optical properties of Mn^{4+} activated $\text{A}_2\text{Ge}_4\text{O}_9$ ($\text{A}=\text{K}, \text{Rb}$) on temperature and chemical environment, *J. Lumin.*, 2016, **177**, 354-360.
10. N. Ma, W. Li, B. Devakumar, Z. Zhang and X. Huang, Finding an efficient far-red-emitting $\text{CaMg}_2\text{La}_2\text{W}_2\text{O}_{12}:\text{Mn}^{4+}$ phosphor toward indoor plant cultivation LED lighting, *Mater. Today Chem.*, 2021, **21**.
11. Y. Wu, D. Lei and C. Wang, The formation of LiAl_5O_8 nanowires from bulk Li-Al alloy enables dendrite-free Li metal batteries, *Mater. Today Phys.*, 2021, **18**.
12. M. G. Brik, I. Sildos, M. Berkowski and A. Suchocki, Spectroscopic and crystal field studies of YAlO_3 single crystals doped with Mn ions, *J. Phys. Condens. Matter*, 2009, **21**, 025404.
13. M. G. Brik, A. M. Srivastava and N. M. Avram, Comparative analysis of crystal field effects and optical spectroscopy of six-coordinated Mn^{4+} ion in the $\text{Y}_2\text{Ti}_2\text{O}_7$ and $\text{Y}_2\text{Sn}_2\text{O}_7$ pyrochlores, *Opt. Mater.*, 2011, **33**, 1671-1676.
14. L. Meng, L. Liang and Y. Wen, Deep red phosphors $\text{SrMgAl}_{10}\text{O}_{17}:\text{Mn}^{4+}$, M (M = Li^+ , Na^+ , K^+ , Cl^-) for warm white light emitting diodes, *J. Mater. Sci. Mater. Electron.*, 2014, **25**, 2676-2681.
15. A. S. Aleksandrovsky, I. A. Gudim, A. S. Krylov and V. L. Temerov, Luminescence of Yttrium Aluminum Borate Single Crystals Doped with Manganese, *Phys. Solid State*, 2007, **49**, 1695-1699.